Partial OH → Me Replacement in the Calixarene Scaffold: Preparation, Conformation, and Stereodynamics of Tetra-*tert*-butyl-25,27-dihydroxy-26,28-dimethylcalix[4]arene and Its Dimethyl Ether Derivative

Joel M. Van Gelder,[†] Jörg Brenn,[‡] Iris Thondorf,*[,‡] and Silvio E. Biali*[,†]

Department of Organic Chemistry, The Hebrew University of Jerusalem, Jerusalem 91904, Israel, and Institut für Biochemie, Fachbereich Biochemie/Biotechnologie, Martin-Luther-Universität Halle-Wittenberg, Kurt-Mothes-Strasse 3, D-06099, Halle, Germany

Received December 19, 1996[⊗]

The first example of the replacement of hydroxyl groups of a calixarene by methyls is described. Reaction of the bis(spirodienone) calixarene derivative **3B** with MeLi afforded the bis addition product **4** which is derived, as shown by X-ray crystallography, from attack on the face of the carbonyls which is *anti* to the ether oxygen. The reaction of the alternant bis(spirodienone) calixarene derivative **3A** with excess MeLi resulted in addition to the C=O groups, but with a concomitant cleavage of the spiro bonds. Ionic hydrogenation (CF_3COOH/Et_3SiH) of this product (**5**) yielded 5,11,17,23-tetra-*tert*-butyl-25,27-dihydroxy-26,28-dimethylcalix[4]arene (**6**) while ionic hydrogenation of **4** resulted in fragmentation of the macrocyclic ring. Calixarene **6** adopts a 1,3-alternate conformation both in solution and in the solid state. **6** is conformationally flexible, and an inversion barrier of 15.1 kcal mol^{-1} was measured for it by DNMR. The dimethyl ether derivative of **6** (i.e., **7**) exists in a partial cone (paco) conformation and undergoes two distinct dynamic processes possessing barriers of 13.3 and 18.1 kcal mol^{-1}. Molecular mechanics calculations predict correctly the preferred conformation of **6** and **7** and indicate that the topomerization pathways resulting in the mutual exchange of the protons within a methylene group are the following: 1,3-alt → paco-(CH_3) → 1,2-alt → paco(CH_3)* → 1,3-alt* for **6,** and paco(CH_3) → 1,3-alt → paco(OCH_3) → 1,2 alt → paco(OCH_3)* →1,3-alt* → paco(CH_3)* for **7** with calculated barriers of 15.0 and 16.1 kcal mol^{-1}, respectively.

Introduction. The calix[*n*]arenes are macrocyclic compounds which are usually obtained by base-catalyzed condensation of *p*-alkylphenols and formaldehyde and are of interest as potential ligands and molecular hosts.[1] One of the most difficult synthetic tasks in calixarene chemistry is to *replace* (rather than to derivatize) the OH groups. There are only few synthetic methodologies capable of replacing a phenolic hydroxyl by another group.[2] At present, only the partial and/or total replacement of the OH groups of calixarenes by H,[3] SH,[4] and NH_2 groups[5] or their formal dehydration to afford xanthene derivatives[5d,6] have been reported. Since the preferred conformation and conformational rigidity of the calixarenes are mainly due to a cyclic array of intramolecular hydrogen bonds ("circular hydrogen bonding"), the replacement of OH groups should influence both the static and dynamic stereochemistries of the resulting systems.

Several [1_4] metacyclophane systems which incorporate *intra*annular methyl groups (e.g., **2a**−**d**) have been described in the literature.[7−10] These compounds were prepared by tetramerization of suitable precursors, and

[†] Hebrew University of Jerusalem.

[‡] Institut für Biochemie.

[⊗] Abstract published in *Advance ACS Abstracts,* May 1, 1997.

(1) For reviews on calixarenes see: (a) Gutsche, C. D. *Calixarenes*; Royal Society of Chemistry: Cambridge, 1989. (b) *Calixarenes: A Versatile Class of Macrocyclic Compounds*; Vicens, J., Böhmer, V., Eds.; Kluwer: Dordrecht, 1991. (c) Böhmer, V. *Angew. Chem., Int. Ed. Engl.* **1995**, *34,* 713. (d) Gutsche, C. D. *Aldrichim. Acta* **1995**, *28,* 1.

(2) (a) According to the "replacement of the hydroxyl group" section of the recent Rodd's *Chemistry of Carbon Compounds* (Tyman, J. H. P. In *Second Supplements to the 2nd Edition of Rodd's Chemistry of Carbon Compounds*; Sainsbury, M., Ed.; Elsevier, Amsterdam, 1996, Volume IIIA, p 247), phenolic hydroxyl groups can be replaced using phosgene in *o*-xylene. As an example, it is stated that 4-hydroxybenzophenone reacts under these conditions, yielding 4-(chlorocarbonyl)-benzophenone. However, the products obtained in the patent cited (BASF AG, DE 384443; *Chem. Abstr.* **1991**, *114,* 6031e) are not the chlorocarbonyls but the corresponding chloroformate derivatives. (b) For a review on hydroxyl replacement in calixarenes see: Biali, S. E. *Isr. J. Chem.,* in press.

(3) See for example: (a) Goren, Z.; Biali, S. E. *J. Chem. Soc., Perkin Trans. 1* **1990**, 1484. (b) Grynszpan, F.; Goren, Z.; Biali, S. E. *J. Org. Chem.* **1991**, *56,* 532. (c) de Vains, J.-B. R.; Pellet-Rostaing, S.; Lamartine, R. *Tetrahedron Lett.* **1994**, *35,* 8147. (d) Harada, T.; Ohseto, F.; Shinkai, S. *Tetrahedron* **1994**, *50,* 13377. (e) Matsuda, K.; Nakamura, N.; Takahashi, K.; Inoue, K.; Koga, N.; Iwamura, H. *J. Am. Chem. Soc.* **1995**, *117,* 5550. (f) For additional synthesis of dehydroxylated calixarenes see: Fukazawa, Y.; Deyama, K.; Usui, S. *Tetrahedron Lett.* **1992**, *33,* 5803. Usui, S.; Deyama, K.; Kinoshita, R.; Odagaki, Y.; Fukazawa, Y. *Tetrahedron Lett.* **1993**, *34,* 8127.

(4) (a) Gibbs, C. G.; Gutsche, C. D. *J. Am. Chem. Soc.* **1993**, *115,* 5338. (b) Ting, Y.; Verboom, W.; Groenen, L. C.; van Loon, J. D.; Reinhoudt, D. N. *J. Chem. Soc., Chem. Commun.* **1990**, 1432. (c) Delaigue, X.; Harrowfield, J. McB.; Hosseini, M. W.; de Cian, A.; Fischer, J.; Kyritsakas, N. *J. Chem. Soc., Chem. Commun.* **1994**, 1579. (d) Delaigue, X.; Hosseini, M. W.; Kyritsakas, N.; de Cian, A.; Fischer, J. *J. Chem. Soc., Chem. Commun.* **1995**, 609. (e) Gibbs, C. G.; Sujeeth, P. K.; Rogers, J. S.; Stanley, G. G.; Krawiec, M.; Watson, W. H.; Gutsche, C. D. *J. Org. Chem.* **1995**, *60,* 8394.

(5) (a) Ohseto, F.; Murakami, H.; Araki, K.; Shinkai, S. *Tetrahedron Lett.* **1992**, *33,* 1217. (b) Aleksiuk, O.; Grynszpan, F.; Biali, S. E. *J. Org. Chem.* **1993**, *58,* 1994. (c) Grynszpan, F.; Aleksiuk, O.; Biali, S. E. *J. Org. Chem.* **1994**, *59,* 2070. (d) Aleksiuk, O.; Cohen, S.; Biali, S. E. *J. Am. Chem. Soc.* **1995**, *117,* 9645.

(6) Diazonium chemistry allowed the preparation of halo- and xanthenocalix[5]arenes: Van Gelder, J. M.; Aleksiuk, O.; Biali, S. E. *J. Org. Chem.* **1996**, *61,* 8419.

(7) Pappalardo, S.; Bottino, F.; Ronsisvalle, G. *Phosphorus Sulfur* **1984**, *19,* 327.

(8) Delaigue, X.; Hosseini, M. W. *Tetrahedron Lett.* **1993**, *34,* 8111.

(9) Pappalardo, S.; Ferguson, G.; Gallagher, J. F. *J. Org. Chem.* **1992**, *57,* 7102.

(10) Schätz, R.; Weber, C.; Schilling, G.; Oeser, T.; Huber-Patz, U.; Irngartinger, H.; von der Lieth, C.-W.; Pipkorn, R. *Liebigs Ann.* **1995**, 1401.

S0022-3263(96)02379-1 CCC: $14.00

for the mesityl calixarene **2c**, it has been concluded that the compound is conformationally rigid.[9] Recent MM3 calculations have predicted that calixarene **2e** possessing *intra*annular methyl groups should only be moderately more rigid than the corresponding OH-substituted systems.[11] In this article we describe a first example of the replacement of phenolic hydroxyl groups of *p-tert*-butylcalix[4]arene (**1**) by an alkyl group (methyl) and an experimental and computational study of the conformation and rotational barriers of the resulting system and its dimethyl ether derivative.

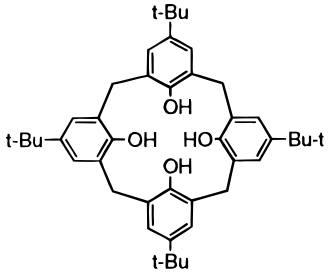

1

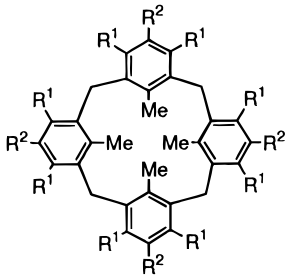

2a R^1 = Me, R^2 = Me
2b R^1 = Me, R^2 = SH
2c R^1 = Me, R^2 = OH
2d R^1 = R^2 = OMe
2e R^1 = H, R^2 = t-Bu

Results and Discussion

Bis(spirodienone) Calixarene Derivatives. Mild oxidation of **1** results in the formation of bis(spirodienone) calixarene derivatives.[12,13] Three isomeric forms are obtained (**3A**, **3A′**, and **3B**) which can be readily separated by chromatography and were characterized by X-ray crystallography.[12] Previous work on monospirodienone calixarene derivatives has shown that their carbonyl group may undergo nucleophilic attack by amino nucleophiles.[5b,d] The reactions of the two major spirodienone products (**3A** and **3B**) with MeLi were therefore studied as a potential route for introducing two methyl groups into the *intra*annular positions of the calixarene scaffold. The addition to the carbonyl groups results in the formation of two new stereocenters. However, it can be expected that the less hindered carbonyl face will be attacked preferentially.

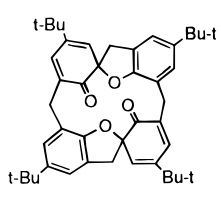

3A *(RS)*
3A' *(RR/SS)*

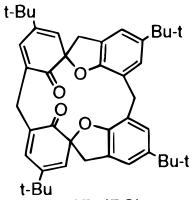

3B *(RS)*

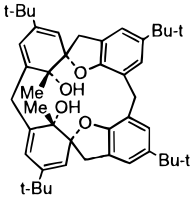

4

Reaction of 3A and 3B with MeLi. Reaction of **3B** with excess MeLi in THF resulted in the formation of a single major product (**4**) as judged by NMR spectroscopy. The ^{13}C NMR displays, in addition to a signal at 92.70 ppm characteristic of the spiro C−O bond, a signal at 75.74 ppm which is ascribed to a C(sp^3)-OH group. The methylene protons display in the ^1H NMR spectrum three pairs of doublets in a 2:2:1:1:1:1 ratio, which are consistent with a structure which retains the C_s symmetry of the starting material. The isolation of a single product indicates that the addition to the carbonyl groups proceeded with high diastereoselectivity. The compound was crystallized from CH_3CN/CH_2Cl_2 and its structure determined by X-ray crystallography. As shown by the crystal structure (Figure 1), **4** is derived from the nucleophilic attack of the MeLi to the *exo* face of the carbonyl groups (*anti* to the spiro oxygens, cf. Scheme 1). The diastereoselectivity of the addition to the carbonyl group is similar to that deduced for the Diels−Alder addition of benzyne to the diene moieties of **3B**.[12] The hydroxyl groups of **4** are oriented in an antiperiplanar arrangement to the methyl groups with one OH group serving as a donor and the second as an acceptor of an intramolecular hydrogen bond.

Reaction of **3A** with 2.2 equivalents of MeLi resulted in an intractable mixture of products. However, the reaction of **3A** with a large excess of MeLi yielded a major product.[14] It displayed two distinct OH signals (7.85 and 2.90 ppm), a pair of doublets for the methylene protons (integrating for four protons) and three signals at 5.97, 6.04, and 6.41 ppm. The last signals were assigned to vinylic protons on the basis of their chemical shifts, and a 2D H−C correlation spectrum which indicated that they

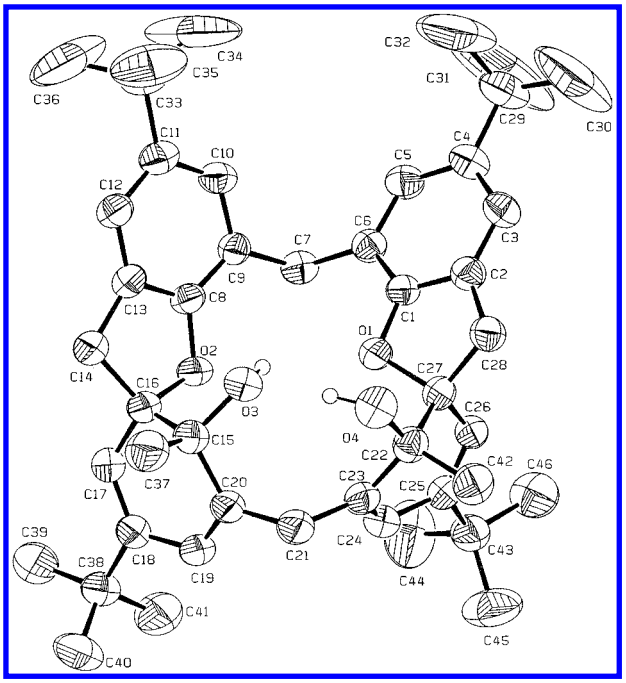

Figure 1. Crystal structure of **4**.

Scheme 1

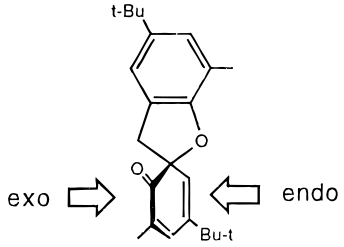

(11) Thondorf, I.; Brenn, J. *J. Mol. Struct. (THEOCHEM)*, in press.
(12) Litwak, A. M.; Grynszpan, F.; Aleksiuk, O.; Cohen, S.; Biali, S. E. *J. Org. Chem.* **1993**, *58*, 393.
(13) For a review on spirodienone calixarene derivatives see: Aleksiuk, O.; Grynszpan, F.; Litwak, M. A.; Biali, S. E. *New J. Chem.* **1996**, *20*, 473.
(14) This product was not detected in the reaction mixture when the reaction was carried out using 2.2 equiv of MeLi in THF.

Scheme 2

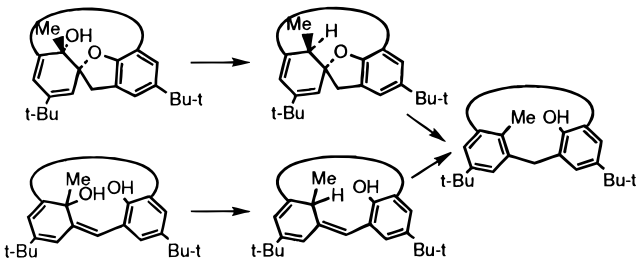

are attached to sp^2 carbons. We assign to this compound formula **5** of either C_i or C_2 symmetry. The formation of **5** can be rationalized assuming that the MeLi acts both as a nucleophile (adding to the carbonyl groups) and as a base (abstracting a methylene proton with the concomitant cleavage of the spiro C−O bonds in an elimination reaction). Calixarene **5** slowly decomposed in solution, and it was used immediately in the next step.

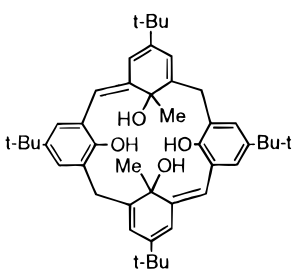

5

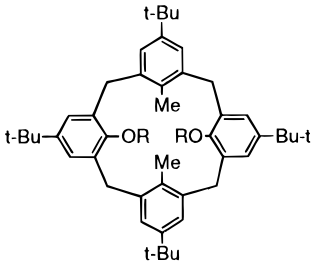

6 R = H
7 R = Me

Ionic Hydrogenation. In principle, both **4** and **5** might be transformed to calixarene systems incorporating proximal or distal *intra*annular methyl groups by reduction of the alcoholic OH groups followed by aromatization (Scheme 2). Indeed, ionic hydrogenation ($CF_3COOH/Et_3SiH/CH_2Cl_2$)[15] of **5** afforded the dimethyldihydroxycalixarene **6** in 35% yield.

In contrast to **5**, treatment of **4** under ionic hydrogenation conditions yielded fragmentation products (**8**−**10**) which were characterized by ^{1}H NMR and by GC-MS.[16] The major product **10** could be isolated from the reaction mixture. These products probably result from the acid catalyzed opening of the spiro bond, followed by migration of the methyl groups and fragmentation. Calixarene **6** was methylated by treatment with NaH/dimethyl sulfate yielding the dimethoxy derivative **7**.

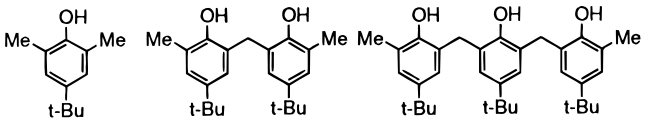

8 **9** **10**

Conformation of Calixarene Systems. The conformation of **1** is usually discussed in terms of four basic conformers resulting from the possible "up"−"down" arrangements of the phenol rings: cone, partial cone (paco), 1,2-alternate (1,2-alt), and 1,3-alternate (1,3-alt) (Chart 1).[1] The preferred conformation of **1** is the cone which is stabilized by a circular array of hydrogen bonds.[1]

Chart 1

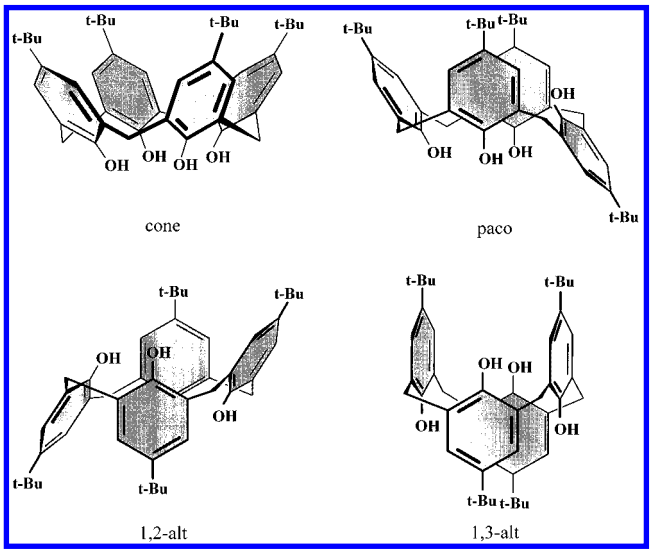

In the case of **6** and **7**, and disregarding the different possible orientations of the hydroxyl or methoxy groups, two distinct paco conformations must be considered in which either the tolyl or the ArOH/ArOMe rings are pointing in opposite directions (i.e., one "up" and one "down").[17] These conformations will be dubbed "paco-(CH_3)" and "paco(OH)"/"paco(OMe)", respectively.

Solution Conformation of 6. The ^{1}H NMR spectrum of **6** at room temperature displays a broad signal for the methylene protons, in agreement with a conformationally mobile structure. At low temperature (400 MHz, $CDCl_3$, 220 K) **6** displays a closely spaced AB system (3.77 and 3.86 ppm) for the methylene protons. The aromatic protons of the tolyl and phenol groups each display a NOESY cross peak with a different methylene proton, in agreement with the presence in solution of a 1,3-alt conformation in which neighboring rings are pointing in opposite directions. This is also supported by the high field chemical shift of the methyl groups (1.31 ppm), indicating that they are under the influence of the shielding effect of the neighboring aryl rings, as expected for a 1,3-alt conformation. A similar solution conformation was deduced for the related dihydroxycalixarene **11**,[18] although in the crystal its methanol solvate exists in a 1,2-alt conformation.[3b] The OH signals of **6** resonate at a higher field (4.04 ppm) as compared with the parent **1** (δ_{OH} 10.2 ppm), as expected, since the disruption of the cyclic array of hydrogen bonds in **1** and the shielding effect of the neighboring rings should result in an upfield shift of these protons.

Crystal Structure of 6. Calixarene **6** was crystallized from CH_2Cl_2/CH_3CN and submitted to X-ray crystallography. The molecule exists in the crystal in a 1,3-alt conformation (Figure 2) in which there is no hydrogen bond between the two distal OH groups. One of the OH groups is nearly coplanar with the corresponding phenol ring, the torsional angle C(20)−C(15)−O(2)−H being 12°. 1,3-Alt conformations have been found in the crystal structures of **2c**[9] and **2d**.[10]

Rotational Barrier of 6. In order to achieve site exchange of the methylene protons all rings must pass through the ring annulus. From the coalescence tem-

(15) Carey, F. A.; Tremper, H. S. *J. Org. Chem.* **1971**, *36*, 758.
(16) For an example of an acid-catalyzed fragmentation of the macrocyclic ring of the monospirodienone derivative of calix[5]arene, see reference 5d.
(17) For identification purposes, the aryl rings of **6** and **7** possessing *intra*annular methyl or methoxy groups will be dubbed "tolyl" and "anisyl", respectively.
(18) Grynszpan, F.; Biali, S. E. *Tetrahedron Lett.* **1991**, *32*, 5155.

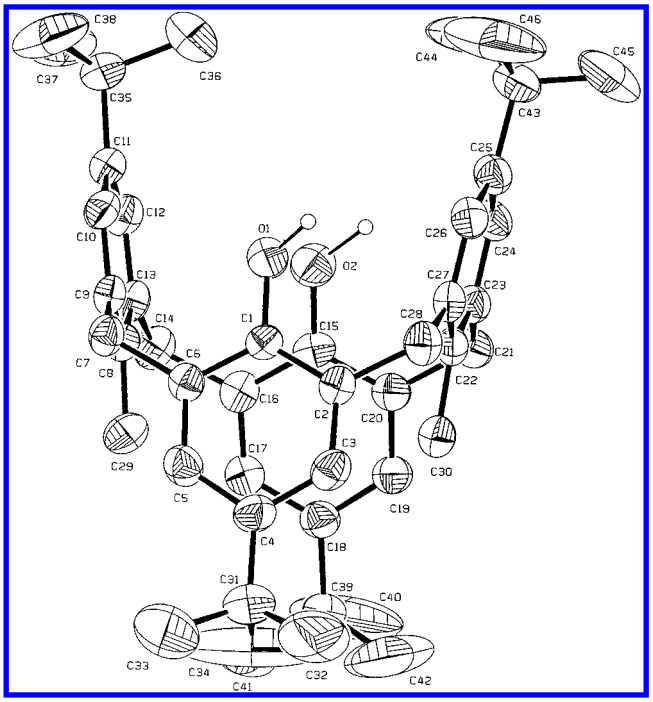

Figure 2. Crystal structure of tetra-*tert*-butyl-25,27-dihydroxy-26,28-dimethylcalix[4]arene (**6**). The large thermal ellipsoids of the methyls of the *tert*-Bu groups are due to rotational disorder of the groups.

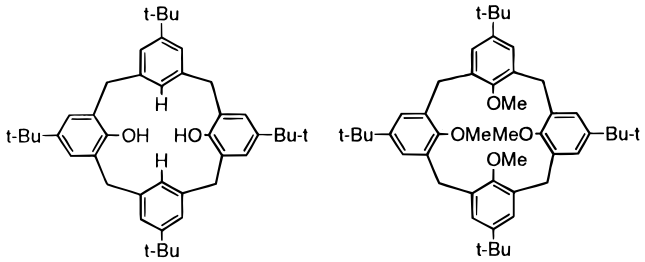

perature of the methylene groups (302 K), the chemical shift difference (35 Hz) and the mutual coupling constant (15.05 Hz) a barrier of 15.1 kcal mol^{-1} was calculated for the 1,3-alt ⇌1,3 alt* exchange in $CDCl_3$.[19] This barrier is comparable to the cone-to-cone inversion barrier of the parent **1** (15.7 kcal mol^{-1} in $CDCl_3$)[20,21] and indicates that the two systems are of comparable flexibility. The absence of circular hydrogen bonding in **1** by the formal OH → Me replacement seems to be compensated by the larger bulk of the methyl groups.

(19) Exchanges rates (k_c) at the coalescence temperatures were calculated according to: Kurland, R. J.; Rubin, M. B.; Wise, W. B. *J. Chem. Phys.* **1964**, *40*, 2426.

(20) Gutsche, C. D.; Bauer, L. J. *J. Am. Chem. Soc.* **1985**, *107*, 6052.

(21) A complete line shape analysis of the temperature dependent ^{1}H NMR of **1** in $CDCl_3$ (Araki, K.; Shinkai, S.; Matsuda, T. *Chem. Lett.* **1989**, 581) provided a $\Delta G_{298}^{\ddagger}$ value of 16.4 kcal mol^{-1}, a value 0.7 kcal mol^{-1} higher than the one (15.7 kcal mol^{-1}) obtained by the coalescence approximation used in ref 20. This is rather puzzling, since the error of the coalescence approximation in the case of **1** (two well resolved singlets in a 1:1 ratio coalescing into a singlet) should be at most 0.1 kcal mol^{-1} (Kost, D.; Carlson, E. H.; Raban, M. *J. Chem. Soc., Chem. Commun.* **1971**, 656). Indeed, in our hands a complete line shape analysis of the temperature dependent ^{1}H NMR of **1** (DNMR5-program) afforded a $\Delta G_c^{\ddagger}$ value identical to the one obtained by the coalescence approximation. We believe that the reason for this discrepancy is that apparently the first simulation was carried out assuming a peak separation according to 1 ppm = 60 Hz instead of 1 ppm = 400 Hz (needed for simulating the ^{1}H NMR spectrum taken with a 400 MHz instrument). Indeed, using the 1 ppm = 60 Hz equivalence we were able to obtain all the (incorrect) lifetimes reported by Araki *et al.*

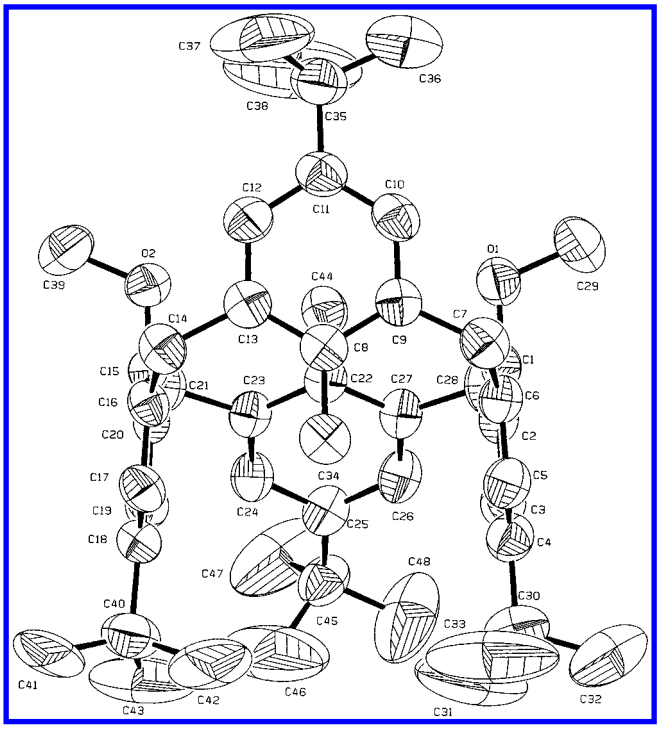

Figure 3. Molecular structure of tetra-*tert*-butyl-25,27-dimethoxy-26,28-dimethylcalix[4]arene (**7**).

Conformation and Stereodynamics of 7. Calixarene **7** displays in the ^{1}H NMR spectrum at low temperature (220 K, $CDCl_3$) four aromatic protons, three t-Bu signals, two pairs of doublets for the methylene signals, and two methyl signals (at 1.40 and 0.70 ppm) while in the ^{13}C NMR spectrum (220 K, $CDCl_3$) 11 aliphatic and 15 aromatic signals are present. This is in agreement with the presence of the paco(CH_3) conformation in which the two tolyl rings are pointing in opposite directions and are bisected by a mirror plane. The high field methyl signal is ascribed to the Me group on the single ring pointing in the opposite direction to the rest, since this methyl is expected to be shielded by the two vicinal anisyl rings. Notably, although the **6** → **7** transformation does not involve the disruption of strong intramolecular hydrogen bonds between the hydroxyl groups, the alkylation changes the conformational preferences of the system.

The structure of a single crystal of **7** grown from CH_2Cl_2/CH_3CN was determined by X-ray crystallography. The molecule adopts also in the crystal the paco(CH_3) conformation (Figure 3) deduced from the solution data in which the methoxy groups are oriented in an "out" fashion. The preferred conformation of the related *p-tert*-butyl-tetramethoxycalix[4]arene **12** is also the paco.[22]

Upon raising the temperature, pairs of aromatic signals, one pair of t-Bu signals, and the two Me signals coalesced while in the methylene region, the two pairs of doublets coalesced and the signals then resharpened

(22) Dhawan, B.; Levine, J. A.; No, K. H.; Bauer, L. J.; Gutsche, C. D. *Tetrahedron* **1983**, *39*, 409. Grootenhuis, P. D. J.; Kollman, P. A.; Groenen, L. C.; Reinhoudt, D.; van Hummel, G. J.; Ugozzoli, F.; Andreetti, G. D. *J. Am. Chem. Soc.* **1990**, *112*, 4165. For calculations on the conformational preferences of **12**, see: Groenen, L. C.; van Loon, J.-D.; Verboom, W.; Harkema, S.; Casnati, A.; Ungaro, R.; Pochini, A.; Ugozzoli, F.; Reinhoudt, D. N. *J. Am. Chem. Soc.* **1991**, *113*, 2385. Harada, T.; Rudzinski, J. M.; Shinkai, S. *J. Chem. Soc., Perkin Trans. 2* **1992**, 2109. Nagasaki, T.; Sisido, K.; Arimura, T.; Shinkai, S. *Tetrahedron* **1992**, *48*, 797. Iwamoto, K.; Ikeda, A.; Araki, K.; Harada, T.; Shinkai, S. *Tetrahedron* **1993**, *49*, 9937.

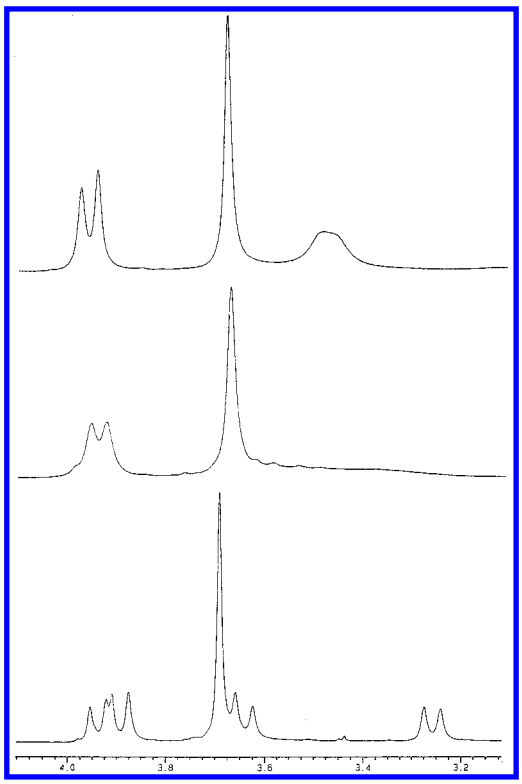

Figure 4. 400 MHz ^{1}H NMR spectra of the methylene protons of **7** (in $CDCl_3$) at different temperatures. From bottom to top: at 230 K, 282 K, and 310 K.

into a pair of doublets (Figure 4). From the frequency difference under slow exchange conditions ($\Delta\nu$ = 120.1, 154.0 Hz) and the coalescence temperature of a pair of aromatic and methylene doublets (T_c = 282 K) a barrier of $\Delta G_c^{\ddagger}$ = 13.3 kcal mol^{-1} ($CDCl_3$) was calculated for the rotational process.[23] The methylene doublets coalesced at 384 K (in $CDCl_2CDCl_2$), yielding a barrier of 18.1 kcal mol^{-1} for the dynamic process. The lower barrier process, which exchanges the two methyl groups, most likely involves the stepwise rotation of the tolyl groups via a symmetric intermediate (i.e., paco(CH_3) → cone → paco(CH_3)* or paco(CH_3) → 1,3-alt → paco(CH_3)*. The process mutually exchanges signals corresponding to the unequivalent methylene groups, and signals on the two tolyl groups, but since the two anisyl rings are not involved in the rotational process the two protons within a given methylene group remain diastereotopic. The high energy process which results in topomerization of the methylene protons must involve the stepwise rotation of all rings through the annulus of the macrocycle.

Exchange with Low-Populated Conformations. In addition, spectral changes were observed in the temperature-dependent NMR of both **6** and **7** which are characteristic of the exchange with a "hidden partner".[24] For example, upon raising the temperature of a $CDCl_3$ solution of **6** at 220 K, the sharp methyl singlet at 1.31 ppm broadened and resharpened at a chemical shift similar to the original one. A similar behavior was observed for the methoxy signal of **7.** This behavior is characteristic of the exchange of the major conformation (1,3-alt and paco(CH_3) for **6** and **7**, respectively) with a second form that cannot be detected by NMR due to its low population. On the basis of the temperature of maximum broadening of the methyl signal and its broadening (284 K and 16.4 Hz, respectively), and assuming that the chemical shift of the methyl group in the second conformation is 2.1 ppm (the "normal" chemical shift for the methyl of a tolyl group), a free energy difference of 1.6 kcal mol^{-1} can be estimated for the energy gap between the 1,3-alt and the low populated conformer of **6** and a barrier of 14.0 kcal mol^{-1} for the diastereomerization process.[25] In principle, two diastereomeric pathways are possible for this process, either involving the rotation of two phenol or two *p*-tolyl groups through the ring annulus. In order to determine the rotational pathways followed by NMR for **6** and **7** we resorted to molecular mechanics calculations.

Interconversion Graph of 6 and 7. The conformations and the barriers for the conformational interconversions of **6** and **7** were calculated with the MM3(92) force field.[26] The calculated relative steric energies of conformers of **6** and **7** and of the transition states for their possible mutual interconversion via single-ring rotations are collected in Tables 1 and 2.

Relative Energies of Conformers of 6 and 7. The calculations predict the relative order of conformational stabilities of **6** as 1,3-alt > paco(OH) > cone > paco(CH_3) > 1,2-alt. The calculations predict correctly that the 1,3-alt is the minimum energy conformation, although the paco(OH) and cone conformers are calculated to lie only 0.2 kcal mol^{-1} above the 1,3-alt form. The cone conformation (of calculated C_2 symmetry) is stabilized by hydrogen bonding between opposite phenol rings. From the two possible paco conformations, the paco(OH) conformer is energetically preferred, due to repulsive van der Waals interactions between the methyl group and the two adjacent hydroxyl groups in the paco(CH_3) conformer.

For **7** the calculations predict the relative order of stabilities paco(CH_3) > 1,3-alt > paco(OCH_3) > cone > 1,2-alt with the 1,3-alt and paco(OCH_3) lying 0.5 and 2.2 kcal mol^{-1} above the paco(CH_3). The most stable cone conformer adopts a C_2 symmetrical arrangement with parallel orientations of the two tolyl rings. In all the conformations calculated, "in" orientations of the methoxy group (i.e., pointing to the molecular cavity) are of higher energy than the "out" arrangements.

The calculations predict correctly the different preferred conformations for **6** and **7**, but seem to underestimate the energy gaps between conformers. In both cases, the calculated geometries are in good agreement with the crystal conformation, with the exception of the $C_{ortho}-C_{ipso}-O-H$ torsional angles of **6** which are pre-

(23) The exchange rates at the coalescence temperature were calculated by the Gutowsky–Holm equation. Gutowsky, H. S.; Holm, C. H. *J. Chem. Phys.* **1956**, *25*, 1228.

(24) Anet, F. A. L.; Basus, V. J. *J. Mag. Reson.* **1978**, *32*, 339. For papers using this method see for example: Adams, S. P.; Whitlock, H. W. *J. Am. Chem. Soc.* **1982**, *104*, 1602. Casarini, D.; Lunazzi, L.; Macciantelli, D. *J. Chem. Soc., Perkin Trans. 2*, **1985**, 1839. For a recent example of the use of this technique for extracting conformational equilibria and rotational barriers of conformational biased calixarene systems, see: Biali, S. E.; Böhmer, V.; Cohen, S.; Ferguson, G.; Grüttner, C.; Grynszpan, F.; Paulus, E. F.; Thondorf, I.; Vogt, W. *J. Am. Chem. Soc.* **1996**, *118*, 12938.

(25) The maximum broadening of a given signal (ω_{max}) is defined as (ω_{obs} - ω_0) where ω_{obs} is the measured maximal line width and ω_0 is the line width in the absence of exchange. ω_{max} is a function of the chemical shift difference of a given group in the exchanging conformations ($\Delta\nu$) and the mole fraction of the less stable conformer (p) p ($\Delta\nu$) = ω_{max} (Hz). At the temperature of maximum broadening (T_m), the rate constant for the conversion of the more stable to the less stable conformer is given by $k = 2\pi p\Delta\nu$ (ref 24).

(26) MM3(92) is available from the Quantum Chemistry Program Exchange, University of Indiana, Bloomington, IN 47405.

Table 1. MM3-Calculated Energies of the Low Energy Conformers and Activation Barriers (relative to the most stable structure) along the Inversion Pathways of 6 (in kcal mol^{-1})

	FSE[a]	ΔE	E_{comp}	E_{bend}	E_{tors}	ΣE_{cross}	ΣE_{vdW}	E_{dipol}
1,3-alt	36.71	**0.00**	6.25	8.09	−34.30	−1.19	39.10	18.76
paco(OH)	36.87	**0.16**	6.23	8.40	−33.17	−1.24	37.84	18.82
cone	36.94	**0.24**	6.41	9.10	−35.01	−1.24	37.59	20.09
paco(CH_3)	38.15	**1.45**	6.81	9.98	−39.30	−1.17	41.90	19.95
1,2-alt	40.57	**3.86**	6.73	11.49	−39.45	−0.99	43.59	19.20
cone ⇌ paco(OH)	44.99	**8.28**	6.55	11.75	−33.81	−0.96	41.67	19.78
cone ⇌ paco(CH_3)	54.96	**18.25**	7.93	12.93	−36.00	−1.06	51.14	20.03
paco(CH_3) ⇌ 1,2-alt	42.97	**6.26**	6.64	10.15	−34.62	−1.16	42.13	19.82
paco(OH) ⇌ 1,2-alt	52.24	**15.53**	7.94	12.21	−36.61	−1.08	50.43	19.35
paco(OH) ⇌ 1,3-alt	45.50	**8.79**	6.52	10.81	−32.57	−0.99	41.98	19.74
paco(CH_3) ⇌ 1,3-alt	51.71	**15.00**	7.71	12.82	−36.98	−0.96	50.01	19.11

[a] FSE = final steric energy; E_{comp} = bond compression energy, E_{bend} = angle bending energy, ΣE_{cross} = sum of the energies from the bend−bend, stretch−bend, and torsion−stretch cross terms, E_{tors} = torsional energy, ΣE_{vdw} = sum of the van der Waals energies, E_{dipol} = dipole-dipole interaction energy.

Table 2. MM3-Calculated Energies of the Low Energy Conformers and Activation Barriers (relative to the most stable structure) along the Inversion Pathways of 7 (in kcal mol^{-1})

	FSE[a]	ΔE	E_{comp}	E_{bend}	E_{tors}	ΣE_{cross}	ΣE_{vdW}	E_{dipol}
paco(CH_3)	42.47	**0.00**	6.40	9.67	−34.03	−1.29	39.83	21.90
1,3-alt	43.02	**0.54**	6.26	9.44	−34.41	−1.20	39.13	23.79
paco(OCH_3)	44.70	**2.23**	6.43	10.09	−34.11	−1.23	39.97	23.55
cone	46.00	**3.53**	6.51	10.31	−33.24	−1.26	40.22	23.46
1,2-alt	46.14	**3.67**	6.30	10.99	−33.02	−1.11	40.85	22.15
cone⇌ paco(OCH_3)	61.86	**19.38**	8.08	10.29	−22.95	−1.33	47.59	20.17
cone⇌ paco(CH_3)	59.09	**16.62**	7.65	14.85	−30.79	−0.96	48.31	20.04
paco(CH_3) ⇌ 1,2-alt	63.26	**20.78**	8.25	11.78	−25.15	−1.18	49.16	20.40
paco(OCH_3) ⇌ 1,2-alt	53.92	**11.45**	7.32	10.99	−30.70	−1.25	46.93	20.64
paco(OCH_3) ⇌ 1,3-alt	58.59	**16.12**	8.49	11.95	−30.24	−1.19	49.71	19.88
paco(CH_3) ⇌ 1,3-alt	57.26	**14.79**	7.41	14.73	−32.17	−0.91	46.87	21.33

[a] For footnotes see Table 1.

dicted to be 90° and in a "in" fashion while in the crystal these angles are 12° and 46°.

Rotational Pathways. The interconversion graphs of the conformers of **6** and **7** via single aryl rotations and the corresponding calculated barriers are displayed in Figures 5 and 6. Additionally, for **7** the rotations of the methoxy groups were also considered. The geometries of the transition states of **6** are very similar to those calculated for other calixarene systems. Thus, the structures of the transition states of the rotations of the phenolic and tolyl rings of **6** resemble those of **1** and **2e**[11] (cf. Figure 7), while the transition states for the rotation of the tolyl rings and anisyl groups of **7** resemble those calculated for **2e**[11] and **12**.[27] In all cases the methoxy group of the rotating ring adopts an "in" orientation. Remarkably, the calculated barriers for the rotation of the methoxy groups are only slightly lower than the ones calculated for the ring rotations. Interestingly, as shown by visual inspection of the structures, the rotation of the methoxy group is accompanied by a simultaneous motion of the calixarene scaffold.

As shown in Figure 5, the rotation of the phenol rings of **6** has a substantially lower barrier than the rotation of the tolyl rings. The rotational pathway of lowest energy (threshold mechanism), which results in the mutual exchange of the methylene protons of **6**, involves the 1,3-alt → paco(CH_3) → 1,2-alt → paco (CH_3)* → 1,3-alt* with a calculated barrier of 15.0 kcal mol^{-1} in excellent agreement with the experimentally determined barrier (15.1 kcal mol^{-1}). For **7** the lowest energy pathway resulting in topomerization of the tolyl rings is paco(CH_3) → 1,3-alt → paco(CH_3)* with a calculated barrier of 14.8 kcal mol^{-1} (experimental value: 13.3 kcal mol^{-1}). According to the calculations, the preferred pathway for mutual exchange of the protons within a methylene group is paco(CH_3) → 1,3-alt → paco(OCH_3) → 1,2-alt → paco(OCH_3)* → 1,3-alt* → paco(CH_3)* with a calculated barrier of 16.1 kcal mol^{-1} (experimental value: 18.1 kcal mol^{-1}). The calculations seem to underestimate the rotational barrier of the anisyl groups, although they indicate that the rotations of the anisyl rings are energetically costlier than the rotation of tolyl rings.

The MM3 calculations indicate that in the case of **6**, even at the lowest temperature examined by NMR, the system should exist as a rapid equilibrium of the 1,3-alt, paco(OH), and cone conformers, the NMR observed being the weighted average of the spectra of the three conformers. The exchange of the 1,3-alt form with a "hidden partner" must correspond to a 1,3-alt ⇌ paco-(CH_3) interconversion.[28] For the case of **7** we ascribe the observed spectral changes to a paco(CH_3) ⇌ cone exchange.

Conclusions. The replacement of two opposite hydroxyl groups of **1** by methyl groups can be achieved via

(27) Fischer, S.; Grootenhuis, P. D. J.; Groenen, L. C.; van Hoorn, W. P.; van Veggel, F. C. J. M.; Reinhoudt, D. N.; Karplus, M. *J. Am. Chem. Soc.* **1995**, *117*, 1611.

(28) There is a discrepancy of ca. 1 kcal mol^{-1} between the barriers extracted from the broadening of the Me signal (exchange with a hidden partner) and the topomerization of the methylene protons (coalescence). This is due to the uncertainty in the chemical shift of the signal of the "hidden" conformer. Moreover, in order to properly compare the rate constants (and barriers) extracted from the two methods a statistical correction factor must be introduced since the first method measures directly the 1,3-alt → paco interconversion, while the second method only follows the molecules in which the two diastereotopic methylene had exchanged magnetic sites. Since the ring inversion process involves a symmetrical intermediate (1,2-alt) which may revert either to "reactant" or "product", half of the molecules which reach that conformation revert to the original 1,3-alt form without topomerization of the methylene protons. The actual rate of the 1,3-alt → paco interconversion (the rate-determining step in the process) is therefore twice the rate derived by the coalescence approximation.

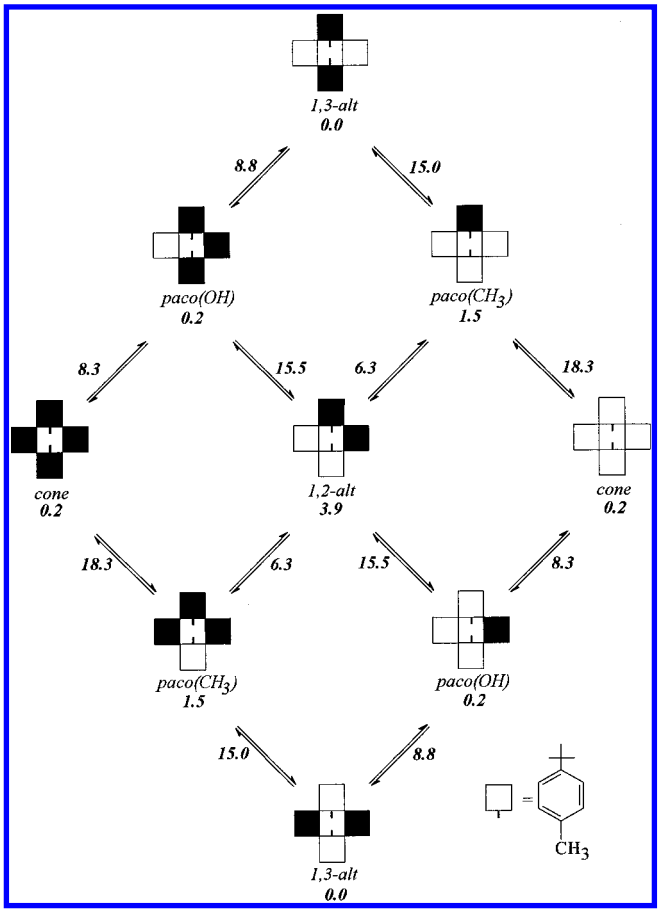

Figure 5. Interconversion graph by single ring rotations of the possible conformers of **6.** Calculated steric energies are relative to the lowest energy conformation (1,3-alt). The peripheral black and white squares represent rings pointing "up" or "down", respectively.

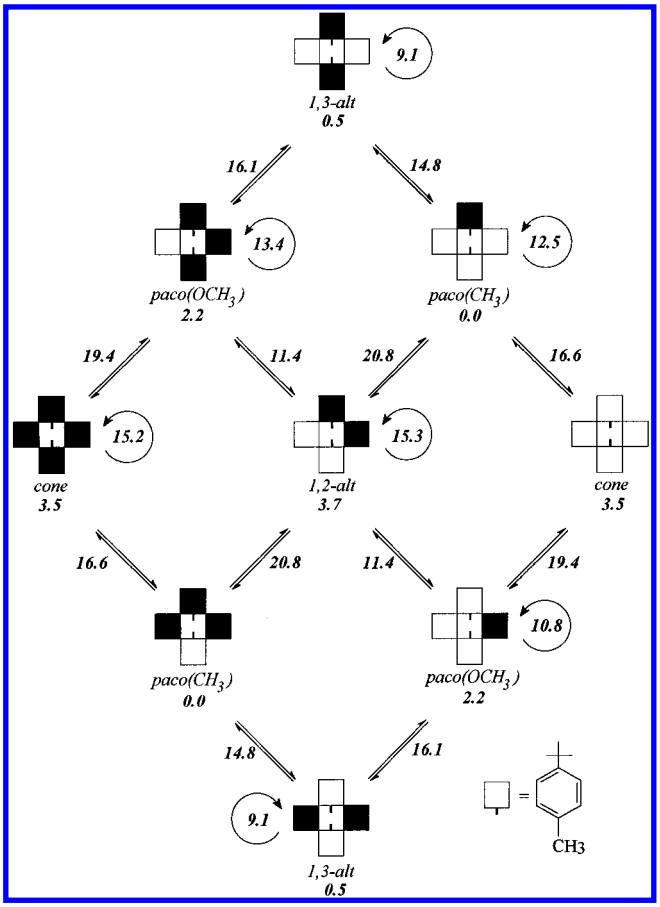

Figure 6. Interconversion graph by single ring rotations of the possible conformers of **7**. Calculated steric energies are relative to the lowest energy conformation (paco(CH_3)). The energies on the curved arrows represent the calculated barriers for the rotation of the methoxy groups relative to the paco-(CH_3) conformation.

the bis(spirodienone) calixarene derivatives. The dihydroxydimethylcalixarene **6** adopts a 1,3-alt conformation while its dimethyl ether derivative prefers the paco(CH_3) form. Both systems are conformationally flexible on the laboratory timescale.

Experimental Section

Molecular Mechanics Calculations. In order to locate the conformational minima on the energy hypersurface, a stochastic search (MM3) was performed for each of the five main conformations of each compound. Starting from the cone conformation of **6** and **7**, the pathways of the conformational interconversion were simulated using the coordinate driver method.[11] For this purpose three methylene carbon atoms were kept fixed in their *z*-coordinates, and ring inversions were performed by modification of the *z*-coordinate of the aromatic *para*-carbon atom in steps of 0.1 Å. The energy minima and maxima were subsequently minimized with the options 6 and 7 of the MM3 force field, respectively, without any constraints. This was followed by full matrix Newton−Raphson minimization of the energy minima and transition states, which were identified by means of their eigenvalues.

The rotations of the methoxy groups were calculated by means of the dihedral driver option of the MM3 program in 5° steps. The rotational barriers were taken directly from the block-diagonal optimization method without location of transition states and full-matrix Newton−Raphson optimization.

A comparison of the energy minimum structures obtained by the stochastic search and by the coordinate driver method indicated that all low energy conformations were found by both methods, the energies differing by a maximum of 0.2 kcal mol^{-1} and the geometries being virtually identical.

Crystallography. The X-ray diffraction data were measured with a ENRAF-NONIUS CAD-4 computer-controlled diffractometer. Cu K_α($\lambda = 1.54178$ Å) radiation with a graphite crystal monochromator in the incident beam was used. All crystallographic computing was done on a VAX 9000 computer using the TEXSAN structure analysis software.[29]

Crystallographic data: **4**: $C_{46}H_{60}O_4 \cdot 0.5CH_3CN$, space group $P\bar{1}$, $a = 14.424(3)$ Å, $b = 16.802(4)$ Å, $c = 9.945(4)$ Å, $\alpha = 100.41(3)°$, $\beta = 91.77(3)°$; $\gamma = 112.38(2)°$, $V = 2179(1)$ Å^3, $z = 2$, $\rho_{calc} = 1.07$ g cm^{-3}, μ(Cu K$_\alpha$) = 4.82 cm^{-1}, no. of unique reflections = 6370, no. of reflections with $I \geq 3\sigma_I = 4986$, $R = 0.085$, $R_w = 0.120$. **6**: $C_{46}H_{60}O_2$, space group $P2_1/n$, $a = 18.593(3)$ Å, $b = 15.778(5)$ Å, $c = 14.325(3)$ Å, $\beta = 102.21(2)°$; $V = 4108(2)$ Å^3, $z = 4$, $\rho_{calc} = 1.04$ g cm^{-3}, μ(Cu K$_\alpha$) = 4.38 cm^{-1}, no. of unique reflections = 6283, no. of reflections with $I \geq 3\sigma_I = 4298$, $R = 0.074$, $R_w = 0.105$. **7**: $C_{48}H_{64}O_2$, space group $P2_1/c$, $a = 14.292(2)$ Å, $b = 15.225(2)$ Å, $c = 20.454(2)$ Å, $\beta = 104.11(1)°$; $V = 4316(1)$ Å^3, $z = 4$, $\rho_{calc} = 1.04$ g cm^{-3}, μ(Cu K$_\alpha$) = 4.33 cm^{-1}, no. of unique reflections = 6682, no. of reflections with $I \geq 3\sigma_I = 4177$, $R = 0.073$, $R_w = 0.099$.

MeLi (1.4 M in ether) was purchased from Aldrich. All reactions with this reagent were performed under nitrogen.

Preparation of 4. To a solution of 1.65 g (2.56 mmol) of **3B** in 300 mL of dry THF at 0 °C was added, with stirring, 13 mL of MeLi (1.4 M in ether, 18.2 mmol). The solution was stirred for 30 min at rt and quenched with 5 mL of H_2O. The solution was extracted with CH_2Cl_2, the phases were sepa-

(29) The authors have deposited atomic coordinates for the structures with the Cambridge Crystallographic Data Centre. The coordinates can be obtained, on request, from the Director, Cambridge Crystallographic Data Centre, 12 Union Road, Cambridge, CB2 1EZ, UK.

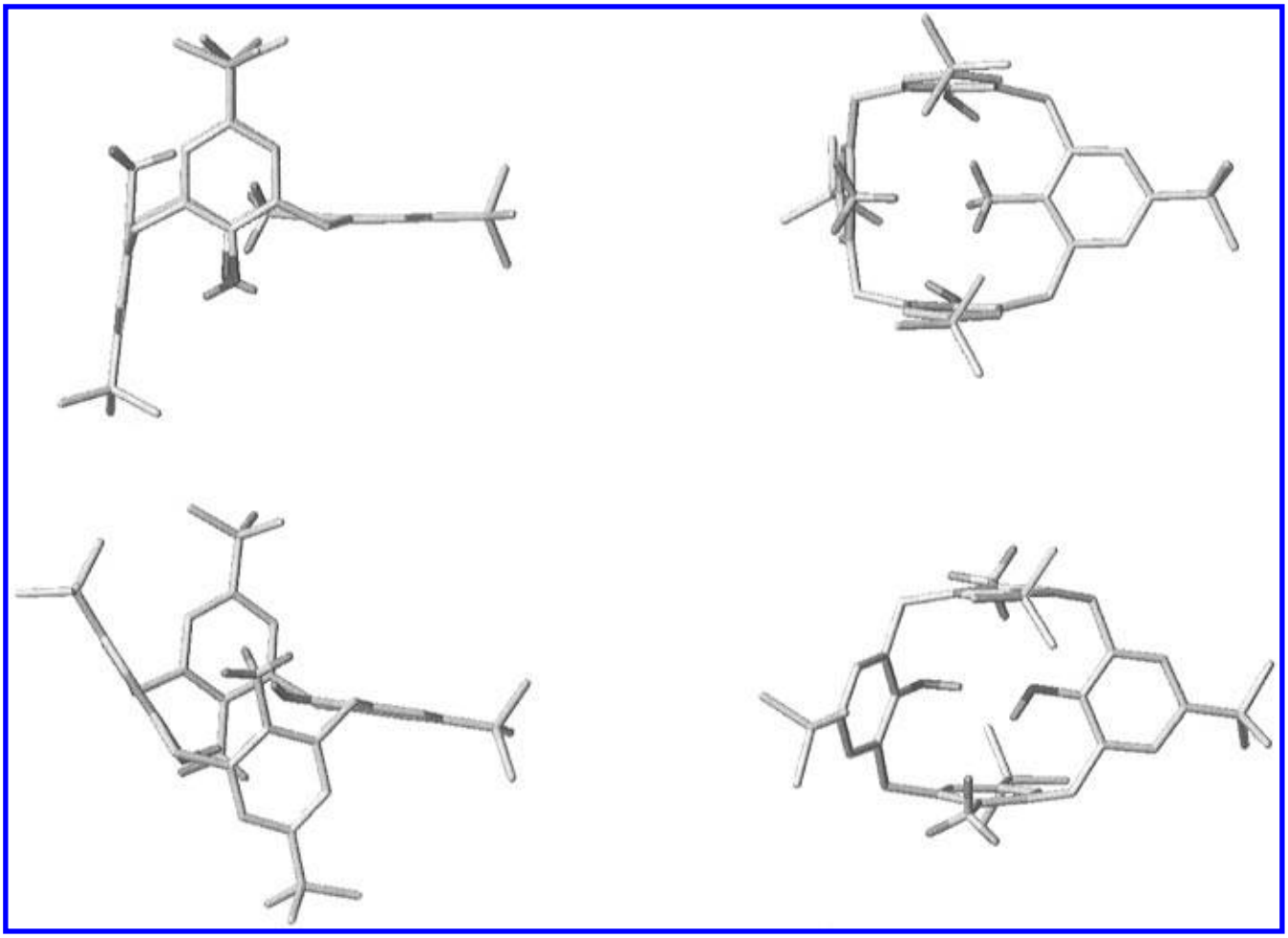

Figure 7. Calculated geometries of the transition states for the 1,3-alt ⇌ paco and paco ⇌1,2-alt conformational interconversions of **6**. Left: side view. Right: top view.

rated, and the organic phase was dried and evaporated. The product was recrystallized from CH_2Cl_2/CH_3CN, yielding 725 mg (42%) of **3B**. Mp: 220−222 °C dec. ^{1}H NMR (400.133 MHz, $CDCl_3$, rt) δ 1.05 (s, 18H, t-Bu), 1.24 (s, 18H, t-Bu), 1.29 (s, 6H, Me), 2.83 (d, J = 13.1 Hz, 1H, CH_2), 2.86 (d, J = 15.6 Hz, 2H, CH_2), 3.23 (d, J = 13.1 Hz, 1H, CH_2), 3.40 (d, J = 13.1 Hz, 1H, CH_2), 3.59 (d, J = 15.5 Hz, 2H, CH_2), 4.06 (d, J = 13.1 Hz, 1H, CH_2), 4.97 (s, 2H, OH), 5.47 (d, J = 1.8 Hz, 2H, C═CH), 5.98 (s, 2H, C═CH), 6.95 (s, 2H, ArH), 7.11 (s, 2H, ArH). ^{13}C NMR (100.62 MHz, $CDCl_3$, rt) δ 22.01, 28.39, 30.22, 31.73, 33.98, 34.19, 35.92, 75.74 (CO), 92.70 (spiro CO), 119.59, 120.56, 120.95, 121.99, 125.28, 126.81, 143.62, 147.64, 148.11, 154.34. CI MS: m/z 677.0 (MH^+)

Reaction of 4 with TFA/Et_3SiH. To a solution of 886 mg (1.31 mmol) of **4** in 30 mL of CH_2Cl_2 at 0 °C was added, with stirring, 6 mL of trifluoroacetic acid (TFA). The color of the solution turned red. Et_3SiH (4 mL) was added (discharging the color of the solution), and the mixture was stirred for 3 h at rt. The solvent was evaporated and the residue analyzed by NMR, which indicated the presence of two main products identified as **9** and **10**. GC MS of the crude product indicated also the presence of 2,6-Me_2-4-*tert*-butylphenol **8** (m/z 178). Trituration of the crude with CH_3CN followed by filtration, yielded 135 mg of pure **10** (21%). Mp: 194−196 °C. ^{1}H NMR (400.133 MHz, $CDCl_3$, rt) δ 1.22 (s, 9H, t-Bu), 1.23 (s, 18H, t-Bu), 2.20 (s, 6H, Me), 3.85 (s, 4H, CH_2), 6.94 (d, 2H, ArH), 7.13 (br s, 4H, ArH), 8.33 (s, 2H, OH (220 K)), 9.44 (s, 1H, OH (220 K)). ^{13}C NMR (100.62 MHz, $CDCl_3$, rt) δ 16.45, 31.45, 31.52, 31.87, 33.93, 33.98, 123.31, 125.18, 125.83, 126.19, 126.25, 127.19, 143.60, 144.24, 147.22, 148.59. CI MS: m/z 502.0 (MH^+). Anal. Calcd for $C_{34}H_{46}O_3$: C, 81.23; H, 9.22. Found: C, 81.80; H, 9.36.

Preparation of 5. To a solution of 1.2 g (1.86 mmol) of **3A** in 400 mL of dry THF at 0 °C was added, with stirring, 12 mL of MeLi (1.4 M in ether, 16.8 mmol). The solution was stirred for 30 min at rt and then quenched by adding 5 mL of H_2O. After evaporation of the solvent, the residue was extracted with ether, dried, and evaporated. The residue was dissolved in MeOH, and the solid which precipitated was filtered yielding 225 mg (18%) of **5**. The compound decomposes in solution. ^{1}H NMR (400.133 MHz, $CDCl_3$, rt) δ 1.13 (s, 18H, t-Bu), 1.26 (s, 18H, t-Bu), 1.38 (s, 6H, Me), 2.90 (s, 2H, OH), 3.10 (d, J = 13.6 Hz, 2H, CH_2), 3.53 (d, J = 13.6 Hz, 2H, CH_2), 5.97 (s, 2H, CH), 6.04 (s, 2H, CH), 6.41 (s, 2H, CH), 6.95 (s, 2H, ArH), 7.06 (s, 2H, ArH), 7.85 (s, 1H, OH). ^{13}C NMR (100.62 MHz, $CDCl_3$, rt) δ 28.83, 31.28, 31.46, 32.70, 33.93, 34.10, 120.76, 121.38, 123.49, 125.95, 126.47, 128.19, 128.94, 143.30, 143.87, 145.21, 145.41, 148.90, 149.12.

Preparation of *p-tert*-Butyl-25,27-dihydroxy-26,28-dimethylcalix[4]arene (6). To a solution of 200 mg (0.30 mmol) of **5** in 30 mL of CH_2Cl_2 was added, with stirring, 2 mL of TFA. The solution turned red, 3 mL of Et_3SiH was added, and the mixture was stirred for 3 h at rt. The solvent was evaporated, and the residue was triturated with CH_3CN and filtered. Recrystallization from CH_2Cl_2/CH_3CN yielded 68 mg of **6** (35%). Mp: 267−269 °C dec. ^{1}H NMR (400.133 MHz, $CDCl_3$, rt) δ 1.23 (s, 36H, t-Bu), 1.39 (br s, 6H, Me), 3.80 (s, 4H, CH_2), 3.84 (s, 4H, CH_2), 4.04 (s, 2H, OH), 7.00 (s, 4H, ArH), 7.17 (s, 4H, ArH). ^{13}C NMR (100.62 MHz, $CDCl_3$, rt) δ 16.80, 29.71, 31.34, 31.44, 33.77, 34.10, 40.69, 126.10, 126.95, 127.22, 133.59, 139.61, 141.52, 148.16, 151.79. CI MS: m/z 645.1 (MH^+). Anal. Calcd for $C_{46}H_{60}O_2$: C, 85.66; H, 9.38. Found: C, 85.38; H, 9.30.

Synthesis of 6 without Isolation of the Intermediate 5. To a solution of 1.2 g (1.86 mmol) of **3A** in 300 mL of dry THF at 0 °C was added, with stirring, 20 mL of MeLi (1.4 M in ether, 28 mmol). The solution was stirred for 30 min at rt, and the reaction was quenched with 5 mL of water. After

evaporating the solvent, the residue was extracted with ether, dried, and evaporated. The crude was dissolved in 50 mL of CH_2Cl_2, 6 mL of TFA and 4 mL of Et_3SiH were added to the red solution, and the mixture was stirred for 3 h at rt. The solvent was evaporated, and the residue was triturated with CH_3CN, yielding 157 mg of **6** (13%).

5,11,17,23-Tetra-*tert*-butyl-25,27-dimethoxy-26,28-dimethylcalix[4]arene (7). To a solution of **6** (75 mg, 0.115 mmol) in 15 mL of dry THF was added NaH (24 mg, 1 mmol). The mixture was heated to reflux, and a solution of dimethyl sulfate (0.1 mL, 1 mmol) in 2 mL of dry THF was added and the reflux continued for 45 min. The excess of NaH was neutralized with EtOH, CH_2Cl_2 was added, and the solution was washed with water. The organic phase was evaporated, and the product was recrystallized from CH_2Cl_2/CH_3CN, yielding 60 mg (77%) of **7**, mp 282−284 °C.

^{1}H NMR (400.133 MHz, $CDCl_3$, 220 K) 0.77 (s, 3H, Me), 0.95 (s, 18H, t-Bu), 1.31 (s, 9H, t-Bu), 1.36 (s, 9H, t-Bu), 1.40 (s, 3H, Me), 3.25 (d, J = 13.0 Hz, 2H, CH_2), 3.64 (d, J = 13.9 Hz, 2H, CH_2), 3.68 (s, 6H, OMe), 3.89 (d, J = 14.3 Hz, 2H, CH_2), 3.96 (d, J = 13.6 Hz, 2H, CH_2), 6.55 (s, 2H, ArH), 6.86 (s, 2H, ArH), 7.08 (s, 2H, ArH), 7.27 (s, 2H, ArH). ^{13}C NMR (100.62 MHz, $CDCl_3$, 220 K) δ 12.78, 16.19, 30.90, 31.17, 31.37, 33.20, 33.53, 33.74, 33.96, 39.37, 61.13, 123.75, 125.14, 125.49, 126.20, 127.11, 131.25, 131.57, 132.02, 134.12, 137.57, 141.34, 143.86, 144.35, 144.66, 153.29. CI MS: m/z 673.2 (MH^+).

Acknowledgment. We thank Dr. Volker Böhmer for helpful discussions, Dr. Shmuel Cohen for the crystal structure determinations, and Dr. Flavio Grynszpan for some preliminary experiments. This research was supported by a grant from the German−Israeli Foundation (GIF) for Scientific Research and Development.

Supporting Information Available: ^{1}H NMR spectra of compounds **4** and **7** (2 pages). This material is contained in libraries on microfiche, immediately follows this article in the microfilm version of the journal, and can be ordered from the ACS; see any current masthead page for ordering information.

JO9623797